MOCVD Growth of Indium Phosphide Nanowire Networks for Thermoelectrics

Amanda Flores

Advisor: Nobuhiko P. Kobayashi

1 Introduction

1.1 Motivation

How could something be manufactured 1000 times smaller than a human hair, and yet still have characteristics alterable at the push of a button? These devices are known as nanowires: conducting or semiconducting wires on the nanometer scale. My research has focused on the study of individual and network nanowires grown through Metal Organic Chemical Vapor Deposition (MOCVD). This is a popular method for nanostructure growth in industry due to its scalability, speed, and control. MOCVD reactors can produce selective area growth for the formation of single nanowires, or they can produce thousands of square centimeters of growth in a single run [1]. Compared to physical deposition processes such as atomic layer deposition, MOCVD is a faster method [2]. Due to the many controllable parameters in MOCVD reactors, they also offer the user control over the output, such as the ideal locations on the substrate for growth, as well as the nanowire's diameter, length, and shape.

One of the first published experiments using the MOCVD process was a thin film growth in 1969 [3]. At this time, the focus was to produce high purity and quality single-crystal materials for semiconductor devices. Chemical Vapor Deposition (CVD) methods had been previously demonstrated, but they required multiple high temperatures in different parts of the process, and multiple steps for the films to be deposited on the actual substrate [4]. H. M. Manasevit's 1969 experiment revolutionized the CVD process by requiring only one high temperature step, and by allowing researchers to grow films directly onto the substrates.

Once MOCVD became a more commonly used technique, different applications were explored. In 1981 injection laser sources in integrated circuits were investigated. These

experiments introduced growth patterns for both circular and striped patterns of thin films [5]. In 1986, MOCVD was explored as a potential option to augment or replace the liquid phase epitaxy method (LPE) used to make semiconductor components for high frequency transistors [6]. It was chosen due to the improved control of composition, production speed, and the thinness of growth layers as compared to LPE. Since then, MOCVD has been used to make more complicated devices, such as superconducting films [7] and thin films designed for solar cells [8].

Recently, thermoelectric devices have been explored as a potential MOCVD growth application. Thermoelectrics are devices which convert a temperature gradient to a voltage difference, known as the Seebeck effect. They can be used as environmentally-friendly power sources, harvesting waste heat and converting it to electrical energy. In 2006, it was estimated that more energy could be gained from available waste heat than all other renewable methods combined. A 2011 Department of Energy study reported that 100 quads of energy were consumed by the United States in the previous year, two-thirds of which were estimated to be lost in conversion, a potential source of waste heat [9]. As a carbon-free green energy source, thermoelectric are the subject of intensified investigations.

1.2 Current Thermoelectric Devices and Challenges

Some thermoelectric devices are currently in use, although not widespread at the level of the general public. 26 NASA space shuttles have contained thermoelectric power sources called radioisotope thermoelectric generators, or RSGs. They are used as power sources for long missions due to their lack of necessary maintenance and long lifetimes; Voyager 1 and 2 each contain 3 RSGs, for an expected operation time of more than 50 years. These devices are powered by radioactive isotopes, where the temperature gradient due to the heat from the

radiating isotopes is used to create energy to fuel the shuttle. However, they are not widely-used to collect waste heat, due to their low efficiency and high production cost; the efficiency of the RSGs used by NASA from the 1960s until 2006 ranged from 6.2-6.8% [10].

1.3 Proposed solution

MOCVD-grown nanostructures are a proposed solution to these challenges. The MOCVD method can be used to grow single-crystal nanostructures on amorphous, or non-single-crystal, substrates. This would allow for cheaper materials such as silicon to be used for substrates, which would be the majority of the material used for the device. Thus, only small amounts of expensive chemicals would be used to fabricate the nanostructures, and the overall price of production would decrease. Due to quantum effects, quasi-1-dimensional nanostructures such as nanowires have a higher efficiency than corresponding bulk materials, as will be discussed in Section 2. Recently, thin films, nanoslabs and nanocolumns of erbium monoantimonide were grown in substrates embedded with nanoparticles, showing a smaller thermal conductivity than identical materials without the nanostructures [11]. This would yield devices potentially both more efficient at converting waste heat to energy, and cheaper to manufacture.

My research hopes to build on these foundations. Our lab focused principally on growing and calculating parameters for indium phosphide and other semiconducting nanowire networks, with an interest in creating thermoelectric devices. We use MOCVD in combination with the vapor liquid solid method, VLS, as will be discussed in a further section. We have worked on optimizing nanowires for use in thermoelectrics, which would require dense, uniform-length networks to make the best possible thermal and electrical contact, but with a large enough length

that the device would not be too easily short-circuited. To design the physical characteristics of our desired structures, we changed parameters such as flow rate of the precursor gases, time at which gases begin/stop flowing, temperature of the reactor throughout the process, and tilting of the sample stage.

In this paper, I will present an overview of the quantum effects that allow nanowires to be useful for our thermoelectric study, a comparison of altered MOCVD parameters on nanowire growth, thermal and optical characterization on these nanowires, and analysis of their potential use in thermoelectric devices. In Section 2, I will discuss quantum-size and finite-size effects, and how they affect our structures. This leads to nanostructures' special thermal and electrical properties, reviewed in Section 3. In Section 4, the growth and characterization methods are explained. In the last section, our progress toward our goal of a working thermoelectric device is discussed.

2 Quantum Effects in Nanowires

Due to their small size, nanowires experience electronic confinement from two sources. The first, known as finite-size or classical effects, occurs when an object is on the order of the mean free path of electrons in the material. At this size, the electrons are confined by the physical edges of the nanowire, resulting in scattering from inner grain and surface boundaries (Fig. 1).

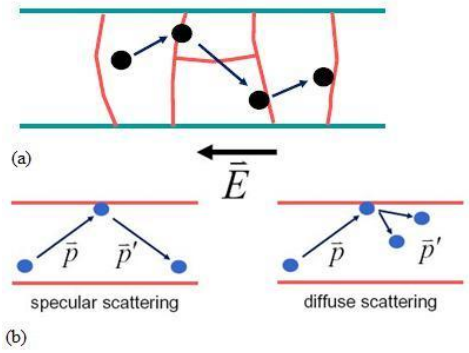

Fig. 1: Scattering within nanowire due to finite-size effects at (a) inner grain boundaries and (b) surface boundaries [12]

Indium phosphide has a mean free path length of 4-32 Å [13], so we can expect to see these finite-size effects in our nanowires. The second is known as quantum-size effects, QE, and these occur for even smaller structures, when the object is on the order of the Fermi wavelength. Equivalently, QE become more prevalent when the electrons within the object have a smaller effective mass m_{eff}. Thus, the low m_{eff} of InP ($.052m_e$) [14], where m_e is the mass of the electron, suggests that QE will occur in our nanowires as well. Experimentally, QE can be observed through photoluminescence spectroscopy, where nanowires of smaller diameters will have blue-shifted peak wavelengths emitted [14].

The density of states (DOS) of a material refers to the number of available energy states per unit volume. This quantity is affected by the dimensionality of the material, from 0-dimensional (quantum dots) to 3-dimensional (bulk materials). Recent experiments have shown that the low dimensionality of nanostructures causes electronic confinement, which contributes to their usefulness as higher-efficiency nanocatalysts [15]. In this section, I will focus on a comparison between the 3-dimensional (3-d) DOS of bulk semiconducting materials and the

quasi-one-dimensional DOS of nanowires, and discuss the benefits nanowires' quasi-one-dimensional DOS brings to devices.

In 3 dimensions, the electrons in a solid are treated as an electron gas. The energy of these electrons consists of purely kinetic energy of the form

$$E = \frac{1}{2}m\boldsymbol{v}^2 = \frac{|\boldsymbol{p}|^2}{2m}$$

where momentum p can be defined as ħk (k is the 3-d wave-number) to obtain the equation

$$E = \frac{\hbar^2\boldsymbol{k}^2}{2m}$$

Constant energy surfaces in three dimensions are thus spherical shells consisting of energies with the same magnitude k-vectors. In the classical case, all energy values would be possible, but quantum mechanically the electrons must obey Schrodinger's equation, which subjects them to boundary restrictions; this requires that the energy of the electrons be discrete. These restrictions require that the wave-number **k** has components

$$k_x = \frac{2\pi n_x}{L}, k_y = \frac{2\pi n_y}{L}, k_z = \frac{2\pi n_z}{L}$$

where n_x, n_y and n_z are integers. The volume taken up in k-space would then be

$$V_{3d} = (\frac{2\pi}{L})^3 \quad (1)$$

To find the DOS, we examine the number of states between 2 spheres in k-space of radius k and k + dk, respectively. The volume between these 2 shells would be

$$4\pi|\boldsymbol{k}|^2 d\boldsymbol{k}$$

Getting the final number of states will simply require us to divide the volume between two shells by the total volume and multiply by 2 for the 2 spin states, resulting in the equation

$$g(k)_{3d}dk = \frac{|k|^2 dk L^3}{\pi^2}$$

Using the previous relation found between energy and k, we find the DOS in 3-d to be

$$g(E)_{3d}dE = \frac{1}{2\pi^2}\left(\frac{2m}{\hbar^2}\right)^{3/2} E^{1/2} dE$$

Thus, we see that the density of states is a function of the square root of the energy (Fig. 2).

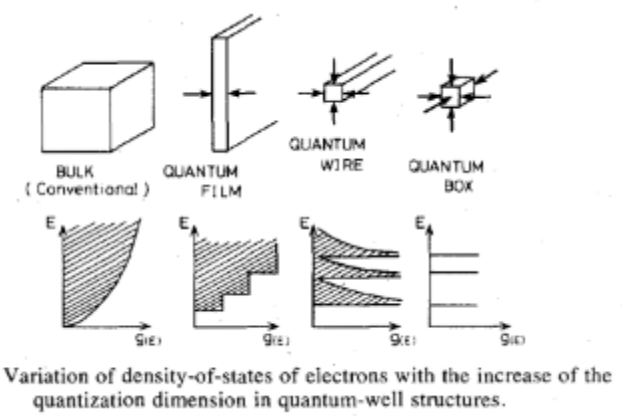

Variation of density-of-states of electrons with the increase of the quantization dimension in quantum-well structures.

Fig. 2: Density of states for 0-, 1-, 2-, and 3- dimensional structures [16]

For the one-dimensional DOS, 2 of our previous k components are fixed, restricting the motion to be in 1 direction. Equation (1) is now reduced to

$$\frac{2\pi}{L}$$

and the constant energy surfaces are now points, with the "volume" between 2 points at k and k + dk expressed as 2dk. Following the same process as in the 3-d case, we find that

$$g(k)_{1d}dk = \frac{2Ldk}{\pi},$$

$$g(E)_{1d}dE = \frac{1}{\pi}\left(\frac{m}{\hbar^2}\right)^{1/2} \frac{1}{E^{1/2}} dE$$

If energy levels beyond the lowest are considered, this equation becomes

$$g(E)_{1d}dE = \frac{1}{\pi}\left(\frac{2m}{\hbar^2}\right)^{1/2} \sum_i \frac{n_i H(E - E_i)}{(E - E_i)^{1/2}} dE,$$

where $H(E-E_i)$ is the Heaviside, or step, function, defined as zero if $E < Ei$, and 1 if $E > Ei$. Thus, it can shown that the 1-d DOS is a function of the reciprocal square root of the energy (Fig. 3).

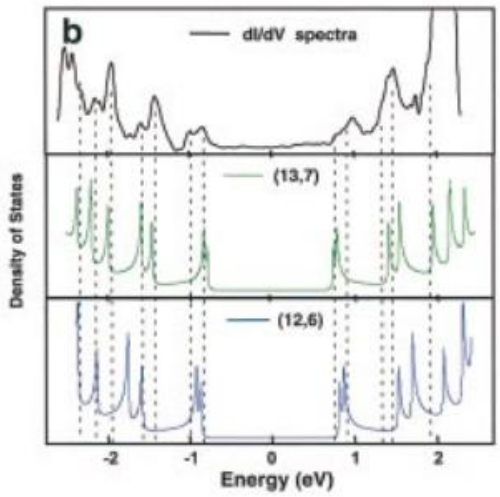

Fig. 3: Top, dI/dV spectra of single-walled carbon nanotubes; middle and bottom, calculated density of states [17]

This difference in the DOS of a quasi-one-dimensional object such as a nanowire and a three-dimensional bulk material results in nanowires having special thermal and electrical properties. Electrons within the nanowires experience quantum confinement, which leads to interesting thermal and electrical properties and makes them ideal for applications such as thermoelectric devices.

3 Thermal and Electrical Properties of Nanowires

The suitability of a material for use in thermoelectric devices can be found from the figure of merit equation,

$$ZT = \frac{\alpha^2 \sigma T}{\kappa} \text{ [18]}.$$

In this equation, α is the Seebeck coefficient of the material, T is the absolute temperature, σ is the electrical conductivity, and κ is the thermal conductivity. The dimensionless quantity ZT is

known as the figure of merit, and the quantity $\alpha^2\sigma$ is known as the power factor. The material coefficient Z can be expressed as a function of lattice thermal conductivity K_L, electronic thermal conductivity K_C, carrier mobility μ and carrier density p as

$$Z = \frac{\alpha^2\sigma}{\kappa_L + \kappa_C} \approx \frac{\alpha^2}{\frac{\kappa_L}{\mu pq} + L_0 T}.$$

Here, q is the charge on the electron and L_0 is the Lorentz number, 1.5E-8 V^2/k^2 for non-degenerate semiconductors [19]. The goal for future thermoelectric devices is to maximize the Z value at room temperature, to make the most efficient devices.

Since the large-scale study of thermoelectric devices began over half a century ago, there has been only a modest increase in the Z value achieved for new alloys. For one popular choice, bismuth telluride, a ZT of .75 at 300K was reported 50 years ago, but in 2001, the most recent bismuth telluride alloy had an improved ZT value of 2.4 at 300K [19]. A universal goal for thermoelectric devices was a ZT of 3 [20], which would allow thermoelectric coolers to economically compete with current technology, but that has not yet become possible with the bulk materials being used today. Many groups are working on making materials with a higher ZT value to make more efficient thermoelectric devices. Initially, it was proposed that decreasing the diameter of the nanowires would increase the power factor without bound [21], due to a relaxation time approximation to the motion of scattered electrons within the material. However, it has since been shown that this approximation was not very accurate in the limit of small nanowire diameters.

It was recently shown that there are limits to the increase of the power factor when the frequency dependent electron scattering mechanisms within the material are considered. When an exact solution to the Boltzmann transport equation was examined, it could be shown that the power factor did increase with decreasing nanowires size, up to a limit. This effect is due to the

large increase in the acoustic phonon-electron scattering that occurs as the nanowire diameter decreases [22]. However, this limiting factor implies that ZT's largest contributing factor is lattice thermal conductivity $K_{L,}$ as opposed to decreased diameter size; thus, the material used for the nanowires is an important choice.

4 Method

4.1 Growth

We use a combination of two methods to epitaxally grow nanowire networks, Metal Organic Chemical Vapor Deposition, MOCVD, and the vapor-liquid-solid method, VLS. The MOCVD apparatus consists of a vacuum pump, a sample chamber, a heating system for the chamber, gaseous precursors, and pipes connecting the components (Fig. 4).

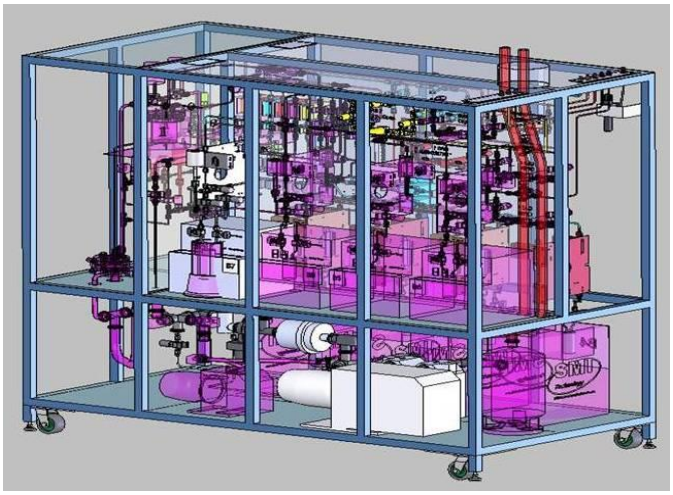

Fig. 4: Schematic of MOCVD used in our experiments

Our MOCVD is plasma-equipped, with a plasma source for better control of the substrate temperature. The substrate can also be heated without plasma using lamps surrounding the chamber, with less control. The entire chamber is a custom design constructed from quartz, which has the benefit of being removable and cleanable, allowing us to use multiple precursor

and dopant combinations if the chamber is properly cleaned between each set. However, quartz is also more easily damaged than stainless steel, the alternative material used.

In the MOCVD method, gaseous precursors containing the desired final elements of the nanowires are flowed into the chamber, trimethyl-indium and tertiary-butyl-phosphine for InP nanowires. The gases flow over a piece of semiconducting material, the substrate. This material has been specially treated with gold droplets prior to the growth; this step is the heart of the VLS method. These droplets, or colloids, can be sputtered on to the substrate and then heated until the gold balls up. Inside the chamber, the temperature is typically above 400 °C, leaving the gold in liquid form. Once the gases reach these colloids, the indium and phosphine are absorbed into the liquid gold until the gold is supersaturated. Lastly, the supersaturated colloids will expel their contents as InP nanowires, growing upward out of the colloids. The colloids can often be observed at the tips of the nanowires after the growth is completed (Fig. 5).

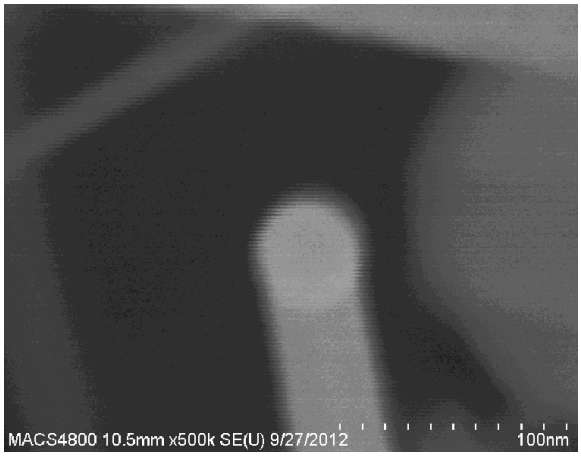

Fig. 5: TEM image of nanowire (photo credit: Kate J. Norris)

The VLS method signifies that metallic colloids have been placed on the substrate to act as a growth catalyst, but the name itself signifies the steps in the nanowire growth process. From vapor-liquid-solid method, vapor is the precursors flowing through in gaseous form, liquid is the

liquid gold catalysts that absorb some components of the vapor, and solid is the nanowires that emerge from the supersaturated colloids.

4.2 Characterization

After the nanowires have been grown, we examine them for defects and take measurements of both optical and thermal characterization quantities. For optical characterization, I used a RPM2000 photoluminescence spectroscopy (PL) mapper to examine our samples for defects. I also used this PL mapper to identify the peak wavelength of light emitted by the sample (Fig. 6) which yields information about the bandgap of the material, the composition of the sample, and the level of quantum confinement within the nanowires.

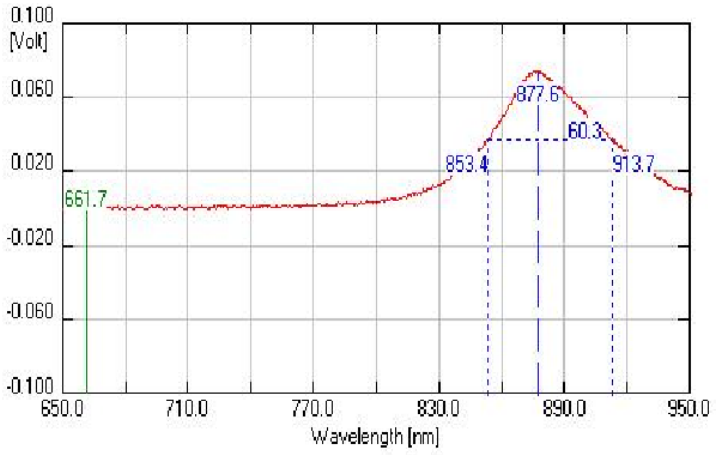

Fig. 6: PL spectra emitted by InP nanowires on silicon, peak wavelength value at 877.6 nm. Taken with RPM2000

This PL mapper had a resolution of approximately .1 mm. We also used a Hitachi S4800 Field Emission scanning electron microscope, SEM, to examine the physical characteristics of our samples. This microscope had a resolution of 1-2 nm, with a maximum magnification of 800,000x. With this SEM, we could measure diameters and lengths of our nanowires, as well as examine the sample closely to discover in which regions nanowires had formed. Lastly, we could refine these measurements using a Hitachi H9500 tunneling electron microscope (TEM), with a

resolution of 1 Å, and a maximum magnification of 1,500,000x. A comparison between images taken by these two microscopes can be seen in Fig. 7.

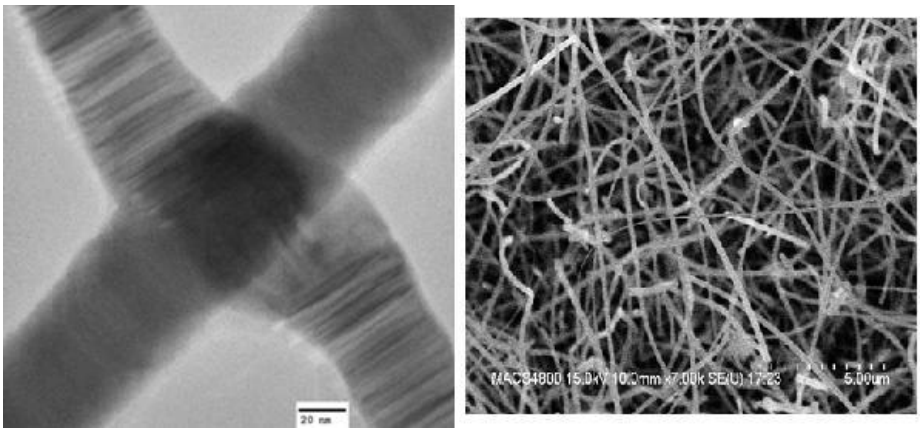

Fig. 7: Left, TEM image of InP nanowires; right, SEM image of InP nanowires. Photo credit: Kate J. Norris

Another important process for nanowire characterization is thermal characterization. We use the comparative cut-bar method to measure Seebeck coefficient, thermal and electrical conductivity, which allows us to find a ZT value for our nanowires. This method does not require a fully functioning device, which allows us to gather measurements on our nanowire networks before our devices are built. Thus, we can optimize our nanowires to have the best qualities for a thermoelectric device, a high Seebeck coefficient, a high electrical conductivity, and a low thermal conductivity. The comparative cut-bar method consists of a heater, a heat sink, two references, and the nanowire sample (Fig. 8).

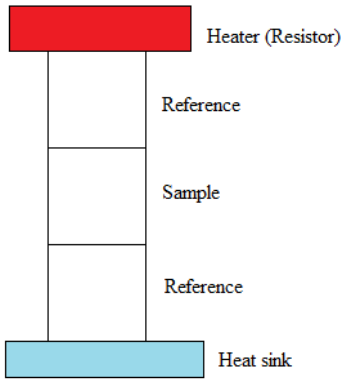

Fig. 8: Comparative cut bar method for thermal characterization of nanowires

In our setup, we use the substrate material as references; thus, if we are measuring InP nanowired on n-type silicon, we use 2 n-type silicon wafers for reference. For a heater, we use a resistor with a current running through it, measuring the temperature the resistor reaches with a thermocouple. Our heat sink is a system attached to the bottom reference to keep the bottom of the apparatus cold. With this system, we can imitate an actual thermoelectric device when we take measurements, allowing us to improve components of a future device.

5 Results

We have successfully grown InP nanowires on many substances, including copper and steel foils. These would be ideal for thermoelectric devices, since they are very flexible and could be formed into cylindrical shapes to offer more surface area to absorb heat. We have also begun characterizing our nanowires both optically and thermally, and are trying to alter growth parameters to obtain the ideal nanowires for our devices. We have found that dense networks of nanowires show a higher electrical conductivity than less dense networks, but we are still working on methods of changing the thermal conductivity and Seebeck coefficient. In the future, we hope to explore the options of plasma-assisted MOCVD to better control the temperature of the substrate during the run, and to expand to different III-IV semiconducting nanowires to find the ideal materials to use to make a working and maximum efficiency thermoelectric device.

References

1. James J. Coleman, "Metalorganic Chemical Vapor Deposition for Optoelectronic Devices," *Proceedings of the IEEE* **85**(11) (1997)

2. Dina H. Triyoso, "Factors Influencing Characteristics of Hafnium Based High-K Dielectrics," *ECS Trans.* **3**(3) pp. 463-477 (2006)

3. H. M. Manasevit, W. I. Simpson, "The Use of Metal-Organics in the Preparation of Semiconductor Materials," *J. Electrochemical Society*. **116**(12), pp. 1725-1732 (1969)

4. James J. Tietjen, James A. Amick, "The Preparation and Properties of Vapor-Deposited Epitaxal $GaAs_{1-x}P_x$ Using Arsine and Phosphine," *J. Electrochemical Society*. **113**(7), pp.724-728 (1966)

5. R. Azoulay, N. Bouadma, J. C. Bouley, L. Dugrand, "Selective MOCVD epitaxy for optoelectronic devices," *J. Crystal Growth*. **55**(1), pp. 229-234 (1981)

6. S.J. Bass, M.S. Skolnick, H. Chudzynska, L. Smith, "MOCVD of Indium Phosphide and Indium Gallium Arsenide Using Trimethyindium-Trimethylamine Adducts," *J. Crystal Growth*. **75**, pp. 221-226 (1986)

7. Hiroshi Ohnishi, Y. Kusakabe, M. Kobayashi, S. Hoshinouchi, H. Harima, K. Tachibana, "Preparation and Characterization of Superconducting Y-Ba-Cu-O Films by the MOCVD Technique," *Japanese J. Appl. Phys*. **29**(6), pp. 1070-1075 (1990)

8. W. W. Wenas, A. Yamada, K. Takahashi, "Electrical and Optical-Properties of Boron-Doped ZnO Thin-Films for Solar-Cells Grown By Metalorganic Chemical Vapor-Deposition," *J. Appl. Phys.* **70**(11), pp. 7119-7123 (1991)

9. U.S. Energy Information Administration, *Annual Energy Review 2011*. Tables 1.1, 1.2, 1.3, 1.4, and 2.1a (2011)

10. Thierry Caillat, P. Gogna, J. Sakamoto, A. Jewell, J. Cheng, R. Blair, J.-P. Fleurial, R. Ewell, "Development of a New Generation of High-Temperature Thermoelectric Unicouples for Space Applications," *Direct Thermal-to-Electrical Energy Conversion ONR/DARPA, San Diego, California, August 29 - September 1* (2006)

11. Kate J. Norris, A. J. Lohn, T. Onishi, E. Coleman, V. Wong, A. Shakouri, G. Tompa, N. P. Kobayashi, "MOCVD Growth of Erbium Monoantiminide Thin Film and Nanocomposites for Thermoelectrics," *J. Electronic Materials*. **41**(5), pp. 971-976 (2012)

12. Thomas W. Cornelius, M. E. Toimil-Molares, "Finite- and Quantum-Size Effects of Bismuth Nanowires," *Nanowires*. Ed. Paola Prete (InTech, 2010)

13. S. Tanuma, C. J. Powell, D. R. Penn, "Calculations of Electron Inelastic Mean Free Paths," *Surface and Interface Analysis*. **17** pp. 927-939 (1991)

14. Mark S. Gudiksen, J. Wang, C. M. Lieber, "Size-Dependent Photoluminescence from Single Indium Phosphide Nanowires," *J. Phys. Chem. B.* **106** pp. 4036-4039 (2002)

15. Lucas F. Seivane, H. Barron, S. Botti, M. A. L. Marques, A. Rubio, X. Lopez-Lozano, "Atomic and electronic properties of quasi-one-dimensional MoS_2 nanowires," *J. Materials Research*. **28**(02) pp. 240-249 (2012)

16. Masahiro Asada, Y. Miyamoto, Y. Suematsu, "Gain and the Threshold of Three-Dimensional Quantum-Box Lasers," *IEEE J. Quantum Electronics.* **22**(9), pp. 1915-1921 (1986)

17. Jiangtao Hu, T. W. Odom, C. M. Lieber, "Chemistry and Physics in One Dimension: Synthesis and Properties of Nanowires and Nanotubes," *Acc. Chem. Res.* **32**, pp. 435-445 (1999)

18. G. S. Nolas, J. Sharp, H. J. Goldsmid, *Thermoelectrics.* (Springer, New York, 2001)

19. Rama Venkatasubramanian, E. Siivola, T. Colpitts, B. O'Quinn, "Thin-film thermoelectric devices with high room-temperature figures of merit," *Nature*. **413** pp. 597-602 (2001)

20. G. Mahan, B. Sales, J. Sharp, "Thermoelectric materials: new approaches to an old problem," *Phys. Today*. **50**(42) pp. 42-47 (1997)

21. L. D. Hicks, M. S. Dresselhaus, "Effect of quantum well structures on the thermoelectric figure of merit," *Phys. Rev. B.* **47**(19) pp. 12727-12731 (1993)

22. D. A. Broido, T. L. Reinecke, "Theory of thermoelectric power factor in quantum well and quantum wire superlattices," *Phys. Rev. B.* **64**(4) (2001)